AIP | Applied Physics Letters

Degradation mechanisms of 2 MeV proton irradiated AlGaN/GaN HEMTs

Jordan D. Greenlee, Petra Specht, Travis J. Anderson, Andrew D. Koehler, Bradley D. Weaver, Martina Luysberg, Oscar D. Dubon, Francis J. Kub, Todd R. Weatherford, and Karl D. Hobart

Citation: Applied Physics Letters **107**, 083504 (2015); doi: 10.1063/1.4929583
View online: http://dx.doi.org/10.1063/1.4929583
View Table of Contents: http://scitation.aip.org/content/aip/journal/apl/107/8?ver=pdfcov
Published by the AIP Publishing

Degradation mechanisms of 2 MeV proton irradiated AlGaN/GaN HEMTs

Jordan D. Greenlee,[1,a)] Petra Specht,[2] Travis J. Anderson,[1] Andrew D. Koehler,[1] Bradley D. Weaver,[1] Martina Luysberg,[3] Oscar D. Dubon,[2] Francis J. Kub,[1] Todd R. Weatherford,[4] and Karl D. Hobart[1]
[1]*U.S. Naval Research Laboratory, 4555 Overlook Ave. SW, Washington, DC 20375, USA*
[2]*University of California at Berkeley, Berkeley, California 94720, USA*
[3]*ERC, Research Center Juelich GmbH, 52425 Juelich, Germany*
[4]*Naval Postgraduate School, Monterey, California 93943, USA*

(Received 22 April 2015; accepted 14 August 2015; published online 26 August 2015)

Proton-induced damage in AlGaN/GaN HEMTs was investigated using energy-dispersive X-ray spectroscopy (EDS) and transmission electron microscopy (TEM), and simulated using a Monte Carlo technique. The results were correlated to electrical degradation using Hall measurements. It was determined by EDS that the interface between GaN and AlGaN in the irradiated HEMT was broadened by 2.2 nm, as estimated by the width of the Al EDS signal compared to the as-grown interface. The simulation results show a similar Al broadening effect. The extent of interfacial roughening was examined using high resolution TEM. At a 2 MeV proton fluence of 6×10^{14} H^+/cm^2, the electrical effects associated with the Al broadening and surface roughening include a degradation of the ON-resistance and a decrease in the electron mobility and 2DEG sheet carrier density by 28.9% and 12.1%, respectively. © *2015 AIP Publishing LLC*.
[http://dx.doi.org/10.1063/1.4929583]

The III-nitride material system has enabled key electronic devices for numerous applications due to its high breakdown field, tunable direct bandgap, adjustable polarization fields, and radiation hardness. For example, AlGaN/GaN high electron mobility transistors (HEMTs) are promising for high power and high frequency applications because of their ability to handle high voltages and currents while also providing low on-resistances.[1] The implementation of AlGaN/GaN HEMTs in conjunction with diamond heat-spreading layers has further widened the possible applications of AlGaN/GaN HEMTs to include high temperature environments.[2] Other extreme environments where AlGaN/GaN HEMTs have shown promise include space, satellite, and military systems, which all require radiation hard devices.

HEMTs operate by modulating a two-dimensional electron gas (2DEG) at the interface between AlGaN and GaN. The number of defects formed in the 2DEG during radiation exposure in these extreme environments is expected to be relatively small because it comprises such a small cross-sectional area of the device. However, defects introduced near the 2DEG are expected to have a significant effect on the operation of the HEMT due to Coulombic scattering.[3] These displacements and their effect on AlGaN/GaN device performance have been previously investigated, and it was determined that radiation-induced displacements can cause acceptor-like defects in the AlGaN layer, which decreases the 2DEG density and electron mobility.[4]

Numerous studies have focused on the degradation of AlGaN/GaN HEMT electronic properties in these extreme environments, but few have focused on the interrelationship between crystalline degradation and electrical degradation.[4–6] In this research, to further understand radiation-induced AlGaN/GaN HEMT degradation, theoretical and physical evidence is correlated to specific radiation-induced defects via transmission electron microscopy (TEM) and energy-dispersive X-ray spectroscopy (EDS). The electrical degradation associated with these radiation-induced defects is also examined.

AlGaN/GaN HEMT devices were fabricated from the following layers: 0.8 μm of unintentionally doped GaN buffer followed by 17.5 nm of $Al_{0.27}Ga_{0.7}N$ grown using metal organic chemical vapor deposition (MOCVD) on a silicon substrate. The devices include mesa isolation and Ti/Al/Ni/Au Ohmic and Ni/Au gate metal stacks, in addition to 100 nm of plasma enhanced chemical vapor deposited SiN_x for surface passivation. Additional details about the device configuration are published elsewhere.[7] The STEM analysis was performed in the ChemiStem at the ERC in Juelich, Germany. The devices were exposed to 2 MeV protons in fluence increments up to 6×10^{14} H^+/cm^2. The space radiation environment includes protons, electrons, heavy ions, and other particles having a wide range of energies. Fortunately, the concept of displacement damage can be used to calculate an equivalent fluence of a monoenergetic beam for ground testing.[8] The fluence increments were chosen to cover a range from the equivalent of a few days in space to about 300 years. The data shown here represent the maximum exposure in order to make the effects more clearly visible. The range of 2 MeV protons in GaN/AlGaN is 24 μm, which is significantly deeper than the thickness of the epitaxial layers. The result of the proton radiation is a uniform distribution of predominatly point defects such as vacancies and interstitials throughout the devices.[9]

In conjunction with the experimental data, computer simulations were performed using the Monte Carlo program "Stopping and Range of Ions in Matter," or SRIM, which is

a)Author to whom correspondence should be addressed. Electronic mail: jordan.greenlee.ctr@nrl.navy.mil

able to accurately calculate stopping energies of energetic ions above 1 MeV to within a few percent for all elemental materials.[10,11] SRIM provided a theoretical preview of the expected Ga, N, and Al displacements in the HEMT structure induced by 2 MeV protons. The results in Fig. 1 show that Al from the AlGaN barrier broadens by 1.75 nm with a simulation uncertainty of 0.5 nm. Similarly, recoils broaden the N and Ga profiles in the AlGaN barrier by 3.0 nm and 0.75 nm, respectively. The penetration depths are set early in the simulation (by 150 000 iterations out of a total 500 000 iterations performed) and henceforth do not increase, suggesting an inherent maximum intermixing depth of Ga, N, and Al in a proton irradiated AlGaN layer. Thus, atomic intermixing of 1–3 nm is expected at the 2DEG (GaN/AlGaN interface). This inherent maximum intermixing depth is due to the maximum recoil energy of a displaced atom being a fixed function of the mass and energy of the incident particle and the target atom mass.[8] Hence, it is reasonable to assume that a fixed maximum energy translates to a fixed maximum knock-on distance.

To obtain physical evidence of this broadening, high resolution STEM and EDS box scans of a cross-section of a HEMT device were performed both on as-grown and post-irradiated devices. The width of each box scan is 15 nm, which was kept constant to ensure that any averaging differences between the as-grown and irradiated EDS scans were equivalent. The STEM scan direction, which correlates with the EDS scans, was towards the surface in the gate region and ran perpendicular to the interfaces. All STEM analysis was performed after irradiation at 6×10^{14} H^+/cm^2. As can be seen in Figs. 2 and 3, the Al profile broadens in the irradiated HEMT compared to the as-grown device. The widths of the Al profiles were determined by comparing the spatial difference between the two points coinciding with half of the steady-state EDS signal in the AlGaN layer. Before radiation, the width of the Al EDS signal is 16.1 nm, while after radiation, it is 18.3 nm. Thus, there was a 2.2 nm broadening in the Al profile, in good agreement with the SRIM results. The broadening of the profile is also accompanied by a change in slope of the Al profile at the interfaces. Before irradiation, the slope of the Al signal at the AlGaN-GaN interface is 20.6 counts/nm. After irradiation, the slope of the Al profile at the AlGaN-GaN interface has decreased to 14.5 counts/nm, further supporting the Al broadening effect. Atomic broadening is also expected to occur at the AlGaN-Ni interface according to the simulation results in Fig. 1. This broadening was confirmed by a decreased Al profile slope at the AlGaN-Ni interface from 34.7 counts/nm before irradiation to 27.5 counts/nm after irradiation. The Al spike in the line scan near the surface after irradiation corresponds to the accumulation at the surface of radiation-damaged amorphous Al.

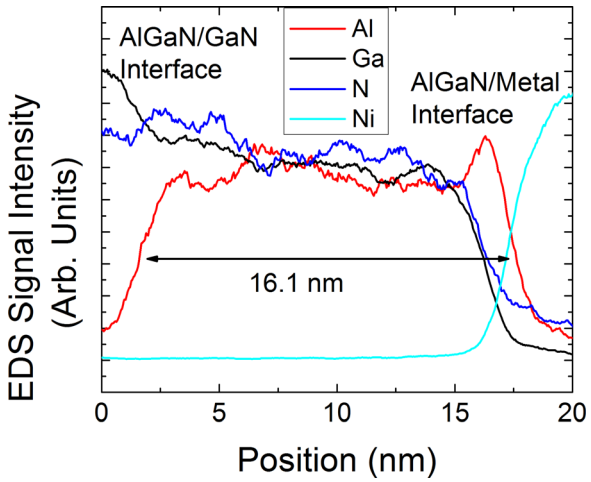

FIG. 2. EDS box scan data through a cross-section of the HEMT before radiation. The width of the Al signal is 16.1 nm.

A previous investigation of Al broadening in an AlGaN/GaN HEMT was performed using 1.8 MeV proton irradiation and secondary ion mass spectroscopy (SIMS).[3] SIMS is known to have spatial resolution limitations that arise from variation in surface morphology and sputter-induced broadening.[3] The radiation-induced atomic broadening produced by 1.8 MeV protons used in the SIMS analysis is expected to

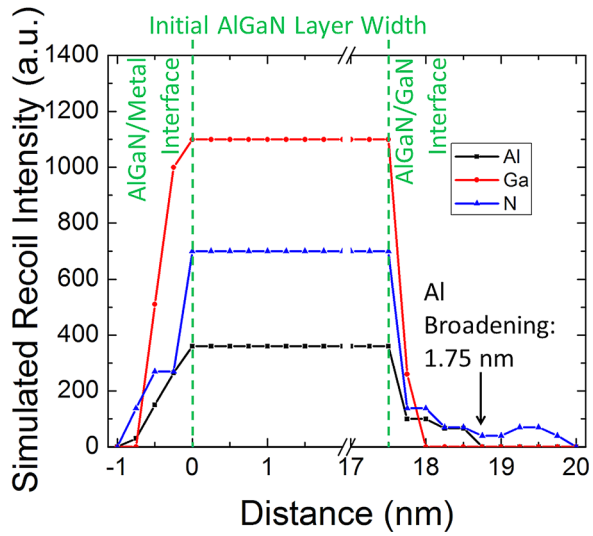

FIG. 1. Simulated recoil distribution of the AlGaN HEMT layer. The Al is broadened by 1.75 nm while the N and Ga atomic profiles are broadened by 3.0 and 0.75 nm, respectively.

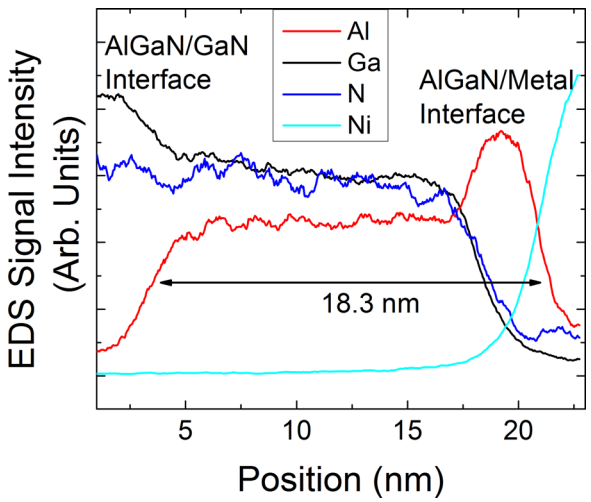

FIG. 3. EDS box scan through a cross-section of the HEMT after a proton radiation dose of $6 \times 10^{14} H^+/cm^2$. The width of the Al signal is 18.3 nm, which is broadened by 2.2 nm compared to the width of the Al signal before radiation.

correspond with a 10% (~0.2 nm) decrease in Al broadening compared to the results reported in this research.[8] It was found in the SIMS investigation that the broadening was ~2.5 nm, which is slightly higher than the results reported herein. In comparison to SIMS, the EDX box scans employed in the present study are not expected to have the same variation that arises from the surface morphology since a cross-section of the sample is being examined, and thus can be used to more reliably determine Al profile information.

As shown in the simulation in Fig. 1 and by the Kinchin-Peace formula,[12] a broadening of the Ga and N are expected to accompany Al broadening. However, since the AlGaN layer is adjacent to a GaN layer, the broadening of Ga and N cannot be resolved but this broadening is expected to additionally contribute to the interfacial roughening and degradation of the electrical properties of the irradiated HEMT.[13] Using high angle annular dark field (HAADF) high resolution STEM, this roughening of the crystalline AlGaN/GaN interface can be further investigated by looking at the Ga column positions. As shown in Fig. 4, before irradiation, the AlGaN/GaN interface is abrupt, a necessary feature for a HEMT with high electron mobility and sheet charge density. In comparison, after irradiation, the interface is less abrupt, with a clear roughening of the interface.

The roughening of the AlGaN/GaN interface and broadening of the Al, Ga, and N concentration profiles in the irradiated HEMTs and their associated defects are expected to degrade the HEMT device performance. The effects that degrade AlGaN/GaN HEMT electrical device performance due to ion irradiation include spontaneous and piezoelectric polarization degradation and AlGaN/GaN interfacial disorder. The broadening of the Al profile and roughening of the AlGaN/GaN interfaces shown in Figs. 3 and 4 have implications for both of these effects.

Radiation induced roughening and the related atomic intermixing/disorder will have a significant impact on the HEMT electrical device performance. The piezoelectric field at the AlGaN/GaN interface is maintained by having an abrupt junction between the AlGaN and GaN. Without the piezoelectric effect, an AlGaN/GaN HEMT is depleted near the interface.[14] The high resolution STEM image comparison shown in Fig. 4 provides direct evidence for interfacial intermixing and roughening which will result in a less abrupt AlGaN/GaN interface and thus begin to deplete the 2DEG. It has also been shown that this interfacial roughening in HEMTs can cause localization of electron levels and a degradation in mobility.[14] The broadening of the Al profile shown in Figs. 2 and 3 will result in the creation of Al vacancies near the 2DEG. The introduction of point defects near the AlGaN/GaN interface results in increased impurity scattering.[3] Al vacancies and vacancy complexes will introduce acceptors in the AlGaN layer and degrade electrical performance, which is consistent with previous simulation and cathodoluminescence spectroscopy studies of irradiated HEMTs.[4,15–17] Ga and N vacancies are expected to accompany the Al vacancies as shown in the SRIM simulation results (Fig. 1), which will also degrade the electrical properties of the HEMT.[13] The combination of atomic intermixing and related surface roughening degraded the 2DEG sheet carrier density and mobility as shown in Fig. 5. This degradation is observed in the irradiated HEMT starting at a fluence of around 1×10^{14} protons/cm^{-2}. After the 6×10^{14} cm^{-2} proton radiation dose, the 2DEG mobility and sheet carrier density decrease by 28.9% and 12.1%, respectively. The degradation in sheet carrier density and mobility mirrors the threshold voltage and drain current in 2 MeV proton-irradiated HEMTs.[7]

In addition to the decrease in 2DEG mobility and sheet carrier density, a degradation in the ON-resistance is observed. The ON-resistance taken under DC and quasistatic pulse conditions degrades following a similar trend to 2DEG mobility and sheet carrier density. However, the ON-resistance degradation under high quiescent drain bias is of a larger magnitude and is initiated at a lower fluence, indicating that this parameter is more sensitive to radiation as shown in Fig. 6. The dynamic ON-resistance measurements are performed by pulsing to the ON-state from OFF-state quiescent points with a drain voltage of 20 V. The threshold voltage is also included in Fig. 6 to provide a comparison of dynamic measurements with a DC device measurement. The large electric field applied during the OFF-state quiescent stress allows electrons to fill additional acceptor-type defect states compared to DC or Hall measurements. A change in

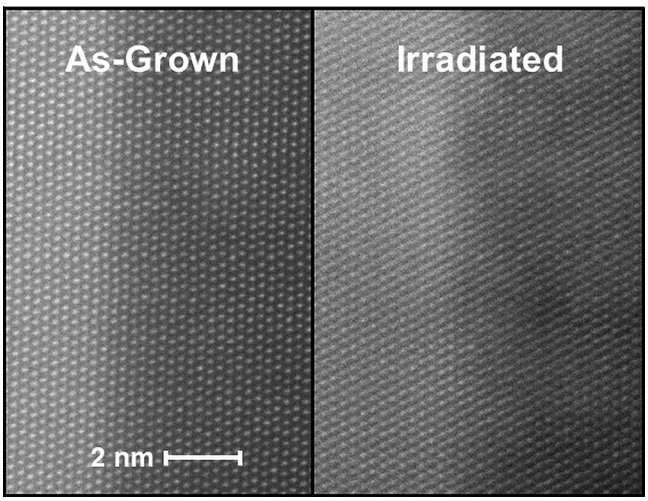

FIG. 4. High resolution STEM image of the GaN/AlGaN interface before (left) and after (right) an irradiation of 6×10^{14} H$^+$/cm^2. The interface is less abrupt after irradiation.

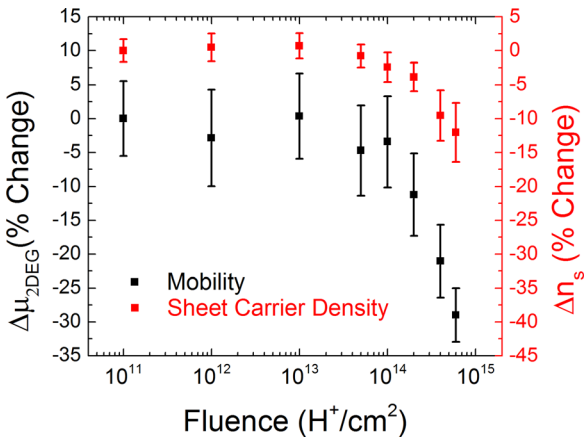

FIG. 5. Hall characteristics as a function of fluence. After a 6×10^{14} cm^{-2} dose of proton radiation, the electron mobility and 2DEG sheet carrier density decrease by 28.9% and 12.1%, respectively.

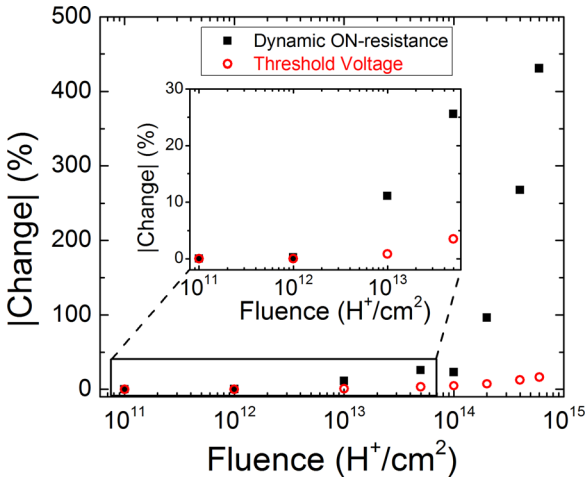

FIG. 6. Dynamic ON-resistance and threshold voltage as a function of fluence. The dynamic ON-resistance is much more sensitive to radiation and demonstrates a greater change at lower fluences compared to DC parameters as shown in the zoomed in portion of the graph (inset).

the dynamic ON-resistance of over 10% is first observed at a dose of 1×10^{13} H^+/cm^2 while the DC parameters, including mobility, sheet carrier density, and threshold voltage, require a dose of over 10^{14} H^+/cm^2 for a similar change. Thus, the dynamic ON-resistance is a significantly more sensitive method to electrically probe the radiation-induced displacement damage observed in this research.[18]

In conclusion, proton damage in AlGaN/GaN HEMTs was simulated, physically investigated, and correlated to electrical degradation. It was determined via EDS that the Al in AlGaN was broadened by 2.2 nm, in good agreement with the simulation results. The resulting interfacial roughening due to displacement damage in the sample was examined using high resolution TEM. The irradiated HEMTs were characterized electrically, and the radiation-induced defects and related interfacial roughening resulted in a decrease in both the electron mobility and 2DEG sheet carrier density of 28.9% and 12.1%, respectively.

Work at NCEM, a facility of the Molecular Foundry, was supported by the Office of Science, Office of Basic Energy Sciences, of the U.S. Department of Energy under Contract No. DE-AC02-05CH11231. This work was supported by the Defense Threat Reduction Agency, DTRA MIPR-HDTRA1412411. This research was performed while J. D. Greenlee held a National Research Council Research Associateship Award at the Naval Research Laboratory. Research at NRL was supported by the Office of Naval Research.

[1]U. K. Mishra, L. Shen, T. E. Kazior, and Y.-F. Wu, Proc. IEEE **96**, 287 (2008).
[2]M. J. Tadjer, T. J. Anderson, K. D. Hobart, T. I. Feygelson, J. D. Caldwell, C. R. Eddy, F. J. Kub, J. E. Butler, B. Pate, and J. Melngailis, IEEE Electron Device Lett. **33**, 23 (2012).
[3]B. D. White, M. Bataiev, S. H. Goss, X. Hu, A. Karmarkar, D. M. Fleetwood, R. D. Schrimpf, W. J. Schaff, and L. J. Brillson, IEEE Trans. Nucl. Sci. **50**, 1934 (2003).
[4]A. Kalavagunta, A. Touboul, L. Shen, R. D. Schrimpf, R. A. Reed, D. M. Fleetwood, R. K. Jain, and U. K. Mishra, IEEE Trans. Nucl. Sci. **55**, 2106 (2008).
[5]B. Luo, J. W. Johnson, F. Ren, K. K. Allums, C. R. Abernathy, S. J. Pearton, R. Dwivedi, T. N. Fogarty, R. Wilkins, A. M. Dabiran, A. M. Wowchack, C. J. Polley, P. P. Chow, and A. G. Baca, Appl. Phys. Lett. **79**, 2196 (2001).
[6]B. Luo, J. W. Johnson, F. Ren, K. K. Allums, C. R. Abernathy, S. J. Pearton, R. Dwivedi, T. N. Fogarty, R. Wilkins, A. M. Dabiran, A. M. Wowchack, C. J. Polley, P. P. Chow, and A. G. Baca, J. Electron. Mater. **31**, 437 (2002).
[7]T. J. Anderson, A. D. Koehler, J. D. Greenlee, B. D. Weaver, M. A. Mastro, J. K. Hite, J. C. R. Eddy, F. J. Kub, and K. D. Hobart, IEEE Electron Device Lett. **35**, 826 (2014).
[8]A. Ionascut-Nedelcescu, C. Carlone, A. Houdayer, H. J. von Bardeleben, J. L. Cantin, and S. Raymond, IEEE Trans. Nucl. Sci. **49**, 2733 (2002).
[9]A. Y. Polyakov, S. Pearton, P. Frenzer, F. Ren, L. Liu, and J. Kim, J. Mater. Chem. C **1**, 877 (2013).
[10]J. F. Ziegler, M. D. Ziegler, and J. P. Biersack, Nucl. Instrum. Methods Phys. Res., Sect. B **268**, 1818 (2010).
[11]J. F. Ziegler, J. Appl. Phys. **85**, 1249 (1999).
[12]G. H. Kinchin and R. S. Pease, Rep. Prog. Phys. **18**, 1 (1955).
[13]E. E. Patrick, M. Choudhury, F. Ren, S. J. Pearton, and M. E. Law, ECS J. Solid State Sci. Technol. **4**, Q21 (2015).
[14]Y. Zhang and J. Singh, J. Appl. Phys. **85**, 587 (1999).
[15]K. B. Nam, M. L. Nakarmi, J. Y. Lin, and H. X. Jiang, Appl. Phys. Lett. **86**, 222108 (2005).
[16]B. D. White, M. Bataiev, L. J. Brillson, B. K. Choi, D. M. Fleetwood, R. D. Schrimpf, S. T. Pantelides, R. W. Dettmer, W. J. Schaff, J. G. Champlain, and U. K. Mishra, IEEE Trans. Nucl. Sci. **49**, 2695 (2002).
[17]S. T. Bradley, A. P. Young, L. J. Brillson, M. J. Murphy, and W. J. Schaff, J. Elecron. Mater. **30**, 123 (2001).
[18]A. D. Koehler, T. J. Anderson, B. D. Weaver, M. J. Tadjer, K. D. Hobart, and F. J. Kub, in *2013 IEEE Workshop on Wide Bandgap Power Devices and Applications (WiPDA)*, Columbus, OH, 2013 (IEEE, 2013), pp. 112.